



## Method of Lines Modeling of Surface Plasmon Modes Excited in Prism-Coupled Configurations

Sujit Chattopadhyay<sup>(1)</sup>, Pradip Kumar Saha<sup>\*(2)</sup>

(1) Indian Telecommunications Service, Department of Telecommunications, Govt. of India, Kolkata, India

(2)(Formerly)Institute of Radiophysics & Electronics, University of Calcutta, Kolkata, India

### Abstract

Dispersion of propagation constants of Surface Plasmon Polariton (SPP) modes at a metal-dielectric interface with the thickness of buffer layer in both the Otto and the Kretschmann-Raether configurations has been modeled using Method of Lines (MOL). The results reaffirm that in either configurations, the excited mode may not have the desired surface plasmon characteristics if the buffer-layer thickness is too small.

### 1. Introduction

Surface Plasmon Polariton (SPP) modes that exist at a metal-dielectric (M-D) interface at visible and IR wavelengths have become a subject of vigorous investigation for the wide range of their prospective applications in photonic integrated circuits and biosensors. Such an interface, which supports only one TM type Surface Electromagnetic Wave (SEW), is the basic guiding structure for SPP. Excitation of SPP constitutes an important segment in the plasmonic research as SPP is not excited by impinging free electromagnetic waves [1]. Two notable excitation schemes for single M-D interface are the Otto [2] and Kretschmann-Raether (K-R) [3] configurations. Both utilize total internal reflection (TIR) at the base of a prism to generate an evanescent field. While the former uses a thin air-gap, the latter uses a thin metal film as the buffer layer. The basic excitation scheme of Otto and K-R configuration are shown in Fig. 1 and Fig. 2 respectively.

In Otto configuration, when  $\theta > \theta_c$  ( $= \sin^{-1} \sqrt{\epsilon_1 / \epsilon_2}$ , where  $\epsilon_1$  and  $\epsilon_2$  are the dielectric constants of the buffer and the prism, respectively), the total internal reflection at the prism base produces an evanescent tail into the buffer layer. Excitation of SPP mode is only possible if the real part of the plasmonic  $\beta$  at the metal – buffer layer interface is equal to  $k_0 \sqrt{\epsilon_2} \sin \theta$  where  $k_0$  is free space wave number. The well known expression for surface plasmon  $\beta$  is  $k_0 \sqrt{\frac{\epsilon_1 \epsilon_M}{\epsilon_1 + \epsilon_M}}$ , for an interface between a dielectric ( $\epsilon_1$ ) half space and a metal ( $\epsilon_M$ ) half space. As such it cannot be applied readily to a practical

configuration as in Fig.1. The precise computation of  $\beta$  for a finite buffer layer thickness and its dispersion with the layer thickness are important for studying the prism excitation of SPP. In this paper we model the waveguide configuration in Fig. 1 as a three-layer structure as shown in Fig. 3(a) and study the dispersion of the plasmonic  $\beta$  and evolution of SPP modes with the thickness of the buffer layer using MOL modeling scheme. A similar study for K-R configuration (Fig. 2) is also carried out using a three-layer model shown in Fig. 3(b). MOL is a highly suitable computational tool for planar geometries. It has been used by Jamid [4] for SP modes on M-D interface. Berini, among others, has extensively applied it in the theoretical study of various plasmonic guides [5].

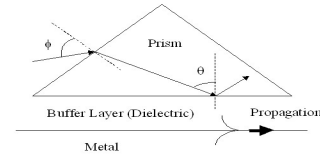


Figure1. SPP excitation in Otto configuration

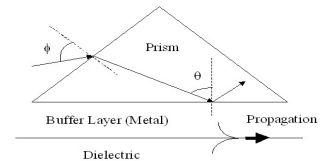
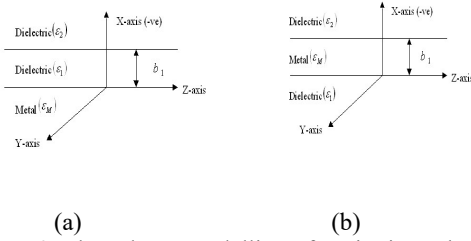


Figure2. SPP excitation in K-R configuration

### 2. Formulation of the problem

The three layer structures in Fig.3(a) and (b) can be considered as representative models of the excitation schemes shown in Fig.1 and Fig. 2, respectively, where the prism is replaced by the bulk dielectric having permittivity  $\epsilon_2$  filling the half space above the buffer layer of finite thickness  $b_1$ . In the computation, the shape of the prism is not important as the physical phenomenon involved in SPP excitation is TIR at the prism base. In case of Otto configuration the buffer layer is a dielectric having permittivity  $\epsilon_1$  whereas for K-R configuration it is

a metal of permittivity  $\epsilon_M$ . The dispersion equations of these three-layer structures involve complex terms because of complex nature of  $\epsilon_M$  and the solutions for  $\beta$  are also complex numbers. Handling such transcendental equations for locating complex roots is usually not straightforward. Generally, the presence of singularity in the equations of multilayer structures and existence of trivial solutions for the equations further complicate the problem. It is also observed that different forms of the dispersion equation resulting from the choice of forms of the trial solutions (exponential, trigonometric or hyperbolic) at different layers, do not always produce results in the entire range of computation. The semi-analytical MOL technique can overcome these difficulties of mode computation.



**Figure 3.** Three-layer modelling of excitation schemes in (a) Fig. 1 and (b) Fig. 2.

## 2.1. Outline of the formulation using MOL

The non-zero field components of the TM type SPP mode in the three-layer structures in Figs. 3(a) and (b) are  $\{E_x, H_y, E_z\}$  and the guiding equation is:

$$\frac{\partial^2 \psi(x, z)}{\partial x^2} + \frac{\partial^2 \psi(x, z)}{\partial z^2} + k_o^2 \epsilon(x) \psi(x, z) = 0 \quad (1)$$

In MOL computation we start with  $\psi(x, z) = H_y$  and then proceed with discretizing the equation (1) along X-axis on a set of parallel lines perpendicular to the X-axis with interval  $\Delta x$  [5]. The parallel lines need not be equidistant and are generally referred as computation gridlines. Incorporating the interface conditions to take care of the boundary conditions at the layer to layer index discontinuities and using 3-point central difference approximation for the term  $\frac{\partial^2 \psi_i(x, z)}{\partial x^2}$  on each gridline  $i$ , we finally arrive at a set of equations that can be expressed in matrix form:  $\bar{Q} \bar{\psi} + \frac{d^2}{dz^2} \bar{\psi} = \bar{0}$  (2)

where  $\bar{Q}$  is an  $M \times M$  square matrix,  $M$  is the total number of gridlines in the geometrical domain of computation and  $\bar{\psi}$  is the column vector containing the discretized field values on the gridlines. The  $M \times M$

$$\text{matrix } \bar{Q} \text{ is expressed as: } \bar{Q} = \frac{1}{(\Delta x)^2} \bar{C} + k_o^2 \bar{N} \quad (3)$$

Where  $\bar{C}$  is a tri-diagonal central-difference matrix with interface conditions incorporated therein [4] and  $\bar{N}$  is a diagonal matrix containing the discretized values of  $\epsilon(x)$  on the gridlines. For particular modal solution of the problem, the  $z$ -dependence of  $\bar{\psi}$  can be expressed as  $\exp(-j\beta z)$ ,  $\beta$  being the propagation constant for the mode. Therefore equation (2) can be further written as:

$$\bar{Q} \bar{\psi} = \beta^2 \bar{\psi} \quad (4)$$

Equation (4) can be solved for the eigen values and the corresponding eigenvectors. The square root of the eigenvalue of the square matrix  $\bar{Q}$  gives the propagation constant and the eigenvector corresponds to the associated discretized field pattern on the gridlines.

## 2.2. Use of perfectly matched layer absorbing boundary condition to restrict the size of computation domain

The problem space under consideration is extended from  $x = -\infty$  to  $x = +\infty$  and therefore the computation domain needs to be restricted to a finite size. Since we have started with  $H_y$  field, the most appropriate termination of the computation window would be to place magnetic walls (MW) at some grid lines on both -ve and +ve X-axis within the Dielectric ( $\epsilon_2$ ) and Metal ( $\epsilon_M$ ) respectively for Otto configuration. Since we are interested in SPP modes, the  $H_y$  field within the metal quickly dies down and therefore a MW at a suitably located grid line in the metal can be safely placed to restrict the domain of computation along +ve X-axis. The situation is not that simple along -ve X-axis. The field pattern in Dielectric ( $\epsilon_2$ ) can have a general characteristic of free propagating wave with no confinement or decay along the -ve X-direction. Therefore placement of a MW on a gridline may generally produce backward reflection resulting in error in computation. To address this issue we have terminated the computation window along -ve X-axis by placing a finite width perfectly matched layer (PML) having absorbing boundary conditions (ABC) [6]. The computation window for Otto configuration using PML and MW is shown in Fig. 4. There is no material discontinuity between the PML and the Dielectric ( $\epsilon_2$ ). However the formulation enforces the wave to travel through a complex distance within the PML by a method of co-ordinate transformation  $x \rightarrow x + j\sigma x$ , ( $\sigma > 0$ ) which causes attenuation of the field inside the PML so that at a suitable grid line  $X = -b_1 - b_2 - b_3$ , a MW can be safely placed. The criteria for deciding the width of the PML, the number of gridlines within the PML and the value of  $\sigma$  have been discussed in detail in [6] and the

same is applied in the present work. The computation window for K-R configuration is shown in Fig. 5. As in Otto configuration, in this case also we have not considered any PML termination for bottom most layer in the computation window and an adequate layer thickness would be enough for computing correct eigenvalues for the desired surface plasmon modes.

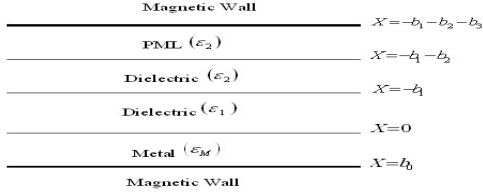


**Figure 4.** Computation window using PML and MW in Otto configuration.

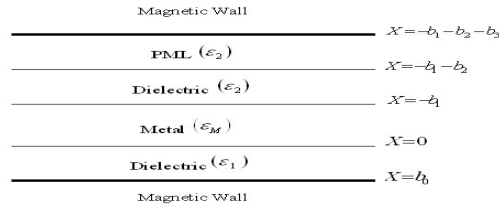


**Figure 5.** Computation window using PML and MW in K-R configuration.

### 3. Results and discussion

The numerical modeling using MOL with PML ABC involves (i) proper choice of discretization scheme of the problem space, (ii) selection of parameters for the PML and (iii) proper identification of the surface plasmon modes from a large set of computed eigenvectors. The model is validated with published results [7] for modified Otto configuration with multilayered buffer dielectric, computed from approximate reflectivity formula. The effective index ( $N_{eff}$ ) of the SPP mode in such a

configuration is defined as  $N_{eff} = \frac{\beta}{k_0}$ , which is a

complex number. The value of effective index for an isolated Dielectric ( $\epsilon_1$ )-Metal ( $\epsilon_M$ ) interface for the chosen parameters is  $2.9553 + j0.0026$ . The computed  $\beta$  is related to the angle of incidence ( $\theta$ ) by the relation:

Real part of  $\beta = \beta_{Real} = k_0 \sqrt{\epsilon_2} \sin \theta$ . To excite SPP at the metal-buffer layer interface, we are therefore interested in finding  $\beta$  in the range:  $k_0 \sqrt{\epsilon_2} \sin \theta_{max} \geq \beta_{Real} \geq k_0 \sqrt{\epsilon_2} \sin \theta_{min}$ . The angles

$\theta_{max}$  and  $\theta_{min}$  correspond to grazing incidence ( $\theta = 90^\circ$ ) and  $\theta_c$  respectively. Therefore, the desired

range of  $\beta_{Real}$  would be  $[k_0 \sqrt{\epsilon_1}, k_0 \sqrt{\epsilon_2}]$ . For the parameters under consideration the range of  $\beta_{Real}$  is  $[2.8577k_0, 3.5k_0]$ . The angle  $\phi$  in the Otto configuration (Fig.1) can be calculated from the value of computed  $\theta$  applying Snell's law. The real and imaginary parts of the computed  $N_{eff}$  for the Otto configuration are plotted against the buffer layer thickness in Fig. 6, with  $\epsilon_M = -125.735 + j3.233$ ,  $\epsilon_1 = 8.1667$ ,  $\epsilon_2 = 12.25$ ,  $\lambda = 1.55 \mu m$ . One notes the departure from the values for the isolated M-D interface: the loss component increases for smaller buffer layer thickness while the real part decreases. The dispersion curves indicate that below a certain buffer layer thickness (about  $0.2 \mu m$  for the present parameters) in Otto configuration, the computed  $\beta$  corresponds to an angle  $\theta$ , which is less than the critical angle at the prism base and the characteristics of the excited mode deviate to a great extent from an ideal surface plasmon mode. We may therefore conclude that to excite SPP at the metal-buffer layer interface in Otto configuration, we cannot arbitrarily reduce the gap between the prism and metal. For larger gap, the computed  $N_{eff}$ , as expected, approaches that of the

isolated Metal-Dielectric (of the buffer layer) interface. But, one cannot in practice make the gap arbitrarily large as it would lead to weaker coupling of SPP through the tunneled evanescent tail generated at prism-buffer layer interface. The dispersion of effective index for K-R scheme for the same set of parameters corresponding to Fig. 6 (Otto) are shown in Fig. 8. In the K-R case, for smaller buffer-layer thickness, both the loss component and the real part of the modal effective index increase. In both the Otto and K-R excitation schemes, the SPP mode is inherently leaky, but with suitable adjustment of the buffer layer thickness it is possible to realize quasi-bound plasmon mode in the metal-dielectric interface. Using the computational windows (Figs. 4 and 5), we studied how the SPP mode evolves as the buffer thickness is varied from very small to large values in both the schemes. From the computed results, we present a few representative plots of the normalized eigen vector ( $H_y$ ) in Fig. 7 (Otto) and 9 (K-R) for two values of buffer thickness in each case. The other parameters are the same as those used in the dispersion diagrams. In both configurations, for the larger buffer thickness, the mode looks like a true SEW with its distinct modal features. Computation with progressively smaller buffer thickness shows that the characteristic modal feature of the SPP gradually diminishes and the SPP mode becomes less tightly bound to the interface because of enhanced coupling of the surface wave with the free electromagnetic wave inside the prism. In both Otto and K-R configurations, the SPP mode becomes lossy (leaky) for very thin buffer thicknesses. However such transition from a quasi-bound to leaky mode takes place at much larger buffer thickness in case of Otto configuration, when compared with K-R configuration. It may be noted that the modal feature of

SPP in K-R configuration resembles that of the dominant asymmetric slow surface plasmon wave in a three-layer D-M-D slab waveguide where the phase velocity decreases with decreasing metal thickness.

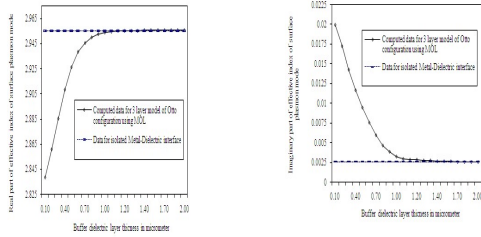


**Figure 6.** Dispersion of real and imaginary parts of  $N_{eff}$  in Otto configuration (Fig.3a)

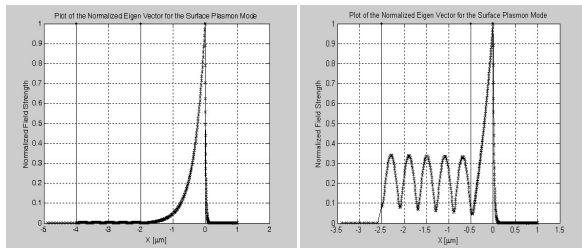


**Figure 7.** Plot of normalized eigen vector ( $H_y$ ) for the SPP mode in the Otto configuration (Fig.3a) for a buffer layer thickness of  $2.00 \mu m$  (left) and  $0.50 \mu m$  (right)

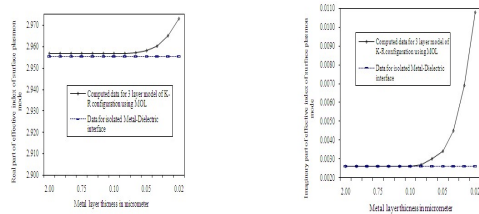


**Figure 8.** Dispersion of real and imaginary parts of surface plasmon mode effective index with metal layer thickness in three-layer K-R configuration (Fig.3b)

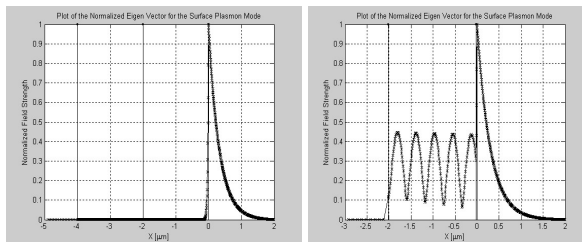


**Figure 9.** Plot of normalized eigen vector ( $H_y$ ) for the SPP mode in the K-R configuration (Fig.3b) for a buffer layer thickness of  $2.00 \mu m$  (left) and  $0.02 \mu m$  (right)

## 4. Conclusions

The criticality of the buffer gap thickness and the loading effect of higher index prism on the surface plasmon mode were studied in [8]. However, the semi analytical method of line modeling scheme, applied to both Otto and K-R configurations, helps in quicker simulation and better understanding of the quality of SPP modes and effect of prism loading. In absence of any empirical relation for the optimum buffer-layer thickness, our study illustrates the utility of MOL for studying the evolution of plasmonic mode with buffer thickness that should be valuable in designing the SPP excitation schemes in photonic integrated circuits. In both the schemes, when the buffer thickness is smaller than a certain value, the mode loses the distinct SPP features. We may also conclude from the nature of dispersion of modal features with buffer layer thickness that K-R configuration would be a preferred excitation scheme compared to Otto configuration in nanophotonics where size minimization is a major concern as the SPP mode becomes weakly bound to the interface at much smaller buffer thickness in K-R configuration.

## 5. References

1. Raether, Heinz, *Surface Plasmons on Smooth and Rough Surfaces and on Gratings* (Vol.111, Springer Tracts in Modern Physics), Springer-Verlag, 1988.
2. Otto, A., "Excitation of nonradiative surface plasma waves in silver by the method of frustrated total reflection," *Z. Phys.* **216**, 398–410 (1968).
3. Kretschmann, E., "Die Bestimmung optischer Konstanten von Metallen durch Anregung von Oberflächenplasmaschwingungen," *Z. Phys.* **241**, 313–324 (1971).
4. Jamid, Hussain A., and Akram, Muhammad Nadeem, "A New Higher Order Finite-Difference approximation Scheme for the Method of Lines", *IEEE Journal of Lightwave Technology*, Vol.19, No.3, 398-404, March 2001.
5. Berini, P., "Plasmon-polariton waves guided by thin lossy metal films of finite width: bound modes of symmetric structures", *Phys. Rev. B* **61**, 10484-10503 (2000)
6. Jamid, H. A., "Frequency-Domain PML Layer Based on the Complex Mapping of Space Boundary Condition Treatment", *IEEE Microwave and Guided Wave Letters*, Vol.10, No.9, 356-358, September 2000.
7. Lee, C. M., Liao, C. H., Chang, L. B., Chiao, T. L., and Tsai, J. H., "Effects of an Air Gap and Prism Dielectric on Properties of Surface Plasma Wave in the Modified Otto Configuration", *Chinese Journal Of Physics*, Vol. 35, No.3, 203-214, June 1997.
8. Sarid, D., "Long-range surface-plasma waves on very thin metal films," *Phys. Rev. Lett.* **47**, 1927–1930 (1981).